The penultimate arginine of the carboxy terminus determines slow desensitization in a P2X receptor from the cattle tick *Boophilus microplus*

Selvan Bavan, Louise Farmer, Shire K. Singh, Volko A. Straub, Felix D. Guerrero and Steven J. Ennion

Department of Cell Physiology and Pharmacology, University of Leicester, Leicester LE1 9HN, UK. (S.B., L.F., S.K.S., V.A.S., S.J.E); USDA-ARS, Knipling Bushland US Livestock Insect Research Laboratory, 2700 Fredericksburg Road, Kerrville, TX 78028, USA. (F.D.G.)

Molecular Pharmacology Fast Forward. Published on January 6, 2011 as DOI: 10.1124/mol.110.070037
This article has not been copyedited and formatted. The final version may differ from this version.

Running Title: *Boophilus microplus* P2X

Corresponding author: Dr Steven J. Ennion

Department of Cell Physiology and Pharmacology,

University of Leicester,

Leicester,

United Kingdom

LE19HN.

Tel: 0116 229 7134.

FAX: 0116-252-5045.

Email: se15@le.ac.uk

Text pages: 32

Tables: 3

Figures: 7

References: 40

Words in Abstract: 250

Words in Introduction: 738

Words in Discussion: 1500

Abbreviations:

EC_{50}, Concentration of agonist evoking 50% of the maximum response.

pEC_{50}, –log10 of the EC_{50} value.

I_{20}, Percent peak current amplitude after 20 seconds of ATP application.

T.10%, Time taken for peak current to decay by 10%.

SNP, Single nucleotide polymorphism.

Molecular Pharmacology Fast Forward. Published on January 6, 2011 as DOI: 10.1124/mol.110.070037
This article has not been copyedited and formatted. The final version may differ from this version.

ABSTRACT

P2X ion channels have been functionally characterized from a range of eukaryotes. Whilst these receptors can be broadly classified into fast and slow desensitizing, the molecular mechanisms underlying current desensitization are not fully understood. Here we describe the characterization of a P2X channel from the cattle tick *Boophilus microplus* (*Bm*P2X) displaying extremely slow current kinetics, little desensitization during ATP application and marked run-down in current amplitude between sequential responses. ATP (EC_{50} 67.1 μM) evoked concentration dependent currents at *Bm*P2X which were antagonized by suramin (IC_{50} 4.8 μM) and potentiated by the antiparasitic drug amitraz. Ivermectin did not potentiate *Bm*P2X currents but the mutation M362L conferred ivermectin sensitivity. To investigate the mechanisms underlying slow desensitization we generated intracellular domain chimeras between *Bm*P2X and the rapidly desensitizing *Hd*P2X receptor from *Hypsibius dujardini*. Exchange of N- or C-termini between these fast and slow desensitizing receptors altered the rate of current desensitization towards that of the donor channel. Truncation of the *Bm*P2X C-terminus identified the penultimate residue (R413) as important for slow desensitization. Removal of positive charge at this position in the mutant R413A resulted in significantly faster desensitization which was further accentuated by the negatively charged substitution R413D. R413A and R413D however still displayed current run-down to sequential ATP application. Mutation to a positive charge (R413K) reconstituted the wild-type phenotype. This study identifies a new determinant of P2X desensitization where positive charge at the end of the C-terminal regulates current flow and further demonstrates that run-down and desensitization are governed by distinct mechanisms.

Molecular Pharmacology Fast Forward. Published on January 6, 2011 as DOI: 10.1124/mol.110.070037
This article has not been copyedited and formatted. The final version may differ from this version.

INTRODUCTION

P2X receptors are extracellular ATP gated ion channels that facilitate the ionotropic component of purinergic signaling (Surprenant and North, 2009). These channels form as homo or heteromeric trimers (Barrera et al., 2005; Nicke et al., 1998) with each monomer consisting of intracellular amino and carboxy termini, two transmembrane domains and a large extracellular region containing five disulfide bonds (Clyne et al., 2002; Ennion and Evans, 2002a) and the agonist binding site (Roberts et al., 2006). The recent determination of the crystal structure of zebrafish P2X4 at 3.1-Å resolution (Kawate et al., 2009) has allowed previous biochemical and mutagenic studies to be interpreted in a structural context (Browne et al., 2010; Young, 2009) and has provided the basis for the commencement of a rudimentary understanding of molecular mechanisms governing aspects of channel function such as ion permeation, channel gating, and agonist/antagonist binding. The zP2X4 structural model however does not include the intracellular N- and C-terminal domains as these were largely removed to aid crystallization (Kawate et al., 2009). It is clear from previous studies that these domains play important roles in regulating P2X channel function, particularly desensitization which manifests itself in two distinct forms. The first, often referred to as “run-down”, is a decline in current amplitude in sequential responses to repeated applications of ATP and has been observed in P2X1,3, 4 and 7 receptors. The second is a decline in current during the continued presence of agonist and is an integral part of the “time course” of an individual response. To avoid confusion, the former will subsequently be referred to as run-down and the latter simply as desensitization. Desensitization of ATP evoked currents in P2X receptors varies between different subtypes and receptors can be broadly classified into those that desensitize very rapidly during the continued presence of agonist, such as P2X1, P2X3 and *Hd*P2X (Bavan et al., 2009), those that display moderate (several seconds) rates of desensitization, including P2X4, P2X5 and most other known invertebrate P2X channels, and those that desensitize slowly such as mammalian P2X2 and P2X7. The molecular mechanisms controlling desensitization are poorly understood and likely multifactorial

Molecular Pharmacology Fast Forward. Published on January 6, 2011 as DOI: 10.1124/mol.110.070037
This article has not been copyedited and formatted. The final version may differ from this version.

involving movement of intracellular, transmembrane and extracellular domains and possibly interactions with other proteins or intracellular messengers (Roberts et al., 2006; Stojilkovic et al., 2005).

Involvement of the transmembrane domains in P2X receptor desensitization was first demonstrated by chimeric P2X1-2 receptors (Werner et al., 1996). Mutation of extracellular domain residues can also profoundly alter current kinetics, for example, mutation of human P2X1 K68, a key residue in the ATP binding site, significantly slows the rate of desensitization (Ennion et al., 2000). Furthermore, chimeric P2X2-3 channels swapping parts of the extracellular domain indicate that the N-terminal half of this domain influences the stability of the desensitized conformation state (Zemkova et al., 2004). The intracellular N-terminal domain also plays a prominent role in regulating desensitization. This region contains a consensus protein kinase C site which is conserved in all known P2X receptors from *Dictyostelium* through to human. Disruption of this site by mutagenesis leads to an increased rate of desensitization in P2X2 (Boue-Grabot et al., 2000) and the already fast desensitizing P2X1 receptor (Ennion and Evans, 2002b). A desensitizing P2X2 splice variant (P2X2b) lacking 69 C-terminal amino acids first demonstrated that the intracellular C-terminal domain can also regulate desensitization (Brandle et al., 1997; Simon et al., 1997) and subsequent mutagenic studies narrowed the functional motif involved to a 6 amino acid region located near the second transmembrane domain (Koshimizu et al., 1998). The juxtamembrane C-terminus region of P2X4 has also been shown to play an important role in desensitization with an aromatic moiety at position 374 and an amino rather than a guanidino group at position 373 being essential for prolonged P2X4 currents (Fountain and North, 2006). Furthermore, exchange of the C-terminal domains in P2X2 and P2X3 receptors results in faster desensitization in P2X2 and slower desensitization in P2X3 (Paukert et al., 2001).

In this current study, we describe a novel invertebrate P2X receptor (*Bm*P2X) cloned from the cattle tick *Boophilus microplus*. This receptor displays extremely slow desensitization properties which we utilize in chimeric and mutagenic studies to identify a new example by which the C-terminal domain can govern P2X receptor desensitization during ATP application by virtue of positive charge at the penultimate position. Our results also further indicate that desensitization during the continued presence of

Molecular Pharmacology Fast Forward. Published on January 6, 2011 as DOI: 10.1124/mol.110.070037
This article has not been copyedited and formatted. The final version may differ from this version.

agonist and run-down of currents between sequential applications are distinct processes regulated by different mechanisms.

Molecular Pharmacology Fast Forward. Published on January 6, 2011 as DOI: 10.1124/mol.110.070037
This article has not been copyedited and formatted. The final version may differ from this version.

MATERIALS AND METHODS

Identification and cloning of a Boophilus microplus P2X receptor. BLAST searches of the GenBank EST database identified partial 5' (accession: CK189412) and 3' (accession: CK189413) sequences from an EST clone (BEACR91) (Guerrero et al., 2005) which showed homology to the vertebrate P2X receptor family. The insert of this clone was sequenced and found to contain an open reading frame of 1242bp. This coding sequence was subsequently subcloned by PCR (Table 1 primer pair 1) into a pcDNA3 based *Xenopus* oocyte expression vector (Agboh et al., 2004) so as to introduce a mammalian Kozak sequence around the start codon. The inclusion of this sequence did not alter the coding sequence of the original clone and has previously been found to aid the expression of non-vertebrate P2X receptors in *Xenopus* oocytes (Agboh et al., 2004). The cloned insert was fully sequenced on both strands using vector and insert specific primers (Automated ABI sequencing service, University of Leicester, U.K.).

Site directed mutagenesis. Point mutations in the *Bm*P2X plasmid were introduced using the QuikChange™ Mutagenesis Kit (Stratagene, U.S.A.) according to the manufacturer's instructions. Methionine at position 362 was mutated to leucine, tyrosine 411 was mutated to alanine and arginine 413 was mutated to lysine, aspartic acid and alanine. A series of truncation mutants were also generated by introducing a premature stop codon (denoted as Δ) at positions 388, 394, 400, 408, 410, 412, 413 and 414. Introduction of the correct mutation and the absence of spontaneous mutations was confirmed by DNA sequencing on both strands.

Generation of BmP2X-HdP2X chimeras. Six chimeric constructs were generated in which one or both of the amino and carboxy intracellular domains of the slow desensitizing *Bm*P2X receptor and the fast desensitizing *Hd*P2X receptor were interchanged (Fig. 3). The positions of transmembrane domains TM1 and TM2 in *Hd*P2X and *Bm*P2X were predicted using TMPred (Hofmann and Stoffel, 1993) and TopPredII (Claros and von Heijne, 1994) programs. Since the two prediction programs varied slightly in assignment of start and end positions for TM domains, the splice residue for cloning was chosen slightly away from the outermost prediction so as to avoid the possibility of disrupting transmembrane sequence.

Molecular Pharmacology Fast Forward. Published on January 6, 2011 as DOI: 10.1124/mol.110.070037
This article has not been copyedited and formatted. The final version may differ from this version.

The N-terminal regions interchanged consisted of residues 1-28 and 1-40 for *Bm*P2X and *Hd*P2X respectively whereas the C-terminal regions consisted of residues 378-414 for *Bm*P2X and 371-480 for *Hd*P2X. Intracellular domains were spliced to residue 29 (N-terminus) and/or residue 377 (C-terminus) in *Bm*P2X and residues 41 and 370 in *Hd*P2X. Chimeras were generated using the technique of seamless cloning. PCR primer pairs (Table 1), one of which incorporated an *EarI* restriction site, an enzyme which cuts outside of its recognition sequence, were designed to allow amplification of the two component parts of the chimera which were subsequently ligated together after *EarI* digestion to produce a seamless join at the desired position. Both wild-type *Bm*P2X and *Hd*P2X sequences contain a single internal *EarI* site and this was disrupted by site directed mutagenesis so as to leave the coding sequence unchanged prior to commencing chimera generation. For chimeras A and C the acceptor wild-type P2X plasmid was first used in a PCR reaction to amplify the sequence from the N-terminus to the end of TM2. The reverse primer incorporates an *EarI* restriction site so that the overhang remaining on the bottom strand after *EarI* digestion of the PCR product corresponds to the inverse complement of the codon at the desired splice position. The C-terminal region from the donor P2X plasmid was amplified in a separate PCR reaction where the forward primer incorporated an *EarI* site that would leave a top strand overhang corresponding to the codon of the splice position. The two *EarI* digested PCR products were subsequently ligated together and blunt end cloned into expression vector. A similar strategy in reverse was used to generate N-terminal exchange chimeras B and D. Chimeras containing a double intracellular domain exchange (E and F) were generated using chimeras B and D respectively as the acceptor sequence. PCR reactions consisted of 10ng plasmid template, 12.5 pmoles each primer, 0.25mM nucleotides, 1x HF buffer (Stratagene) and 1.25 units *PfuUltra*™ DNA polymerase (Stratagene). Thermal cycling consisted of 95 ^{o}C for 2 minutes followed by 20 cycles of 95^{o}C for 30 s, 55 ^{o}C for 30 sec and 72^{o}C for 1 min 10 sec. All chimeric constructs were verified by sequencing on both strands.

Electrophysiological recordings. Sense strand cRNA was generated from linearized P2X plasmids using a T7 mMessage mMachine^{TM} kit (Ambion, U.S.A.). Manually defolliculated stage V *Xenopus* oocytes were injected with 50ng cRNA and stored at 18^{o}C in ND96 buffer (96 mM NaCl, 2 mM

Molecular Pharmacology Fast Forward. Published on January 6, 2011 as DOI: 10.1124/mol.110.070037
This article has not been copyedited and formatted. The final version may differ from this version.

KCl, 1.8 mM $CaCl_2$, 1 mM $MgCl_2$, 5 mM sodium pyruvate, 5 mM HEPES, pH 7.6) prior to recording 3-7 days later. Two-electrode voltage clamp recordings were made from P2X expressing *Xenopus* oocytes at room temperature using an Axoclamp 900A amplifier with a Digidata 1440A data acquisition system and pClamp 10 acquisition software (Molecular Devices U.S.A.). Oocytes were clamped at -60 mV and recording solution consisted of ND96 with $BaCl_2$ (1.8mM) substituting $CaCl_2$ in order to prevent the activation of endogenous oocyte calcium activated chloride channels. Microelectrodes were filled with 3 M KCl and had a resistance of 0.2 MΩ. ATP was applied from a nearby U-tube perfusion system whereas suramin (Bayer, U.K.), ivermectin and amitraz were bath perfused and also present at the appropriate concentration in the U-tube application of ATP. In order to control for the run-down in responses displayed by *Bm*P2X between sequential applications of ATP, concentration response data were normalized to a bracketing concentration of 100 μM ATP applied prior to and subsequent to the test concentration with a five minute recovery period between applications. Current properties were analyzed using Clampfit 10.2 software (Molecular Devices USA.). Desensitization in wild-type, chimeric and mutant channels was quantified using the parameters of I_{20} (% peak current amplitude after 20 seconds of ATP application) and T.10% (time taken for peak current to decay by 10%). T.10% was chosen rather than the more conventional T.50% since wild-type and some mutant channel currents did not decay by 50% even after prolonged (up to 6 minutes tested) application of agonist. Run-down was quantified by recording peak amplitudes after sequential ATP applications with a five minute recovery period between the end of one application and the start of the next. Data are presented as mean ± S.E.M. Differences between means were tested using one way analysis of variance (Kruskal-Wallis) with Dunn's multiple comparison post test (Graphpad Prism software). Concentration response data were fitted with the equation $Y = ((X)^H.M)/((X)^H + (EC_{50})^H)$ where Y = response, X = agonist concentration, H is the Hill coefficient, M is maximum response and EC_{50} is the concentration of agonist evoking 50% of the maximum response. pEC_{50} is the –log10 of the EC_{50} value.

Unless otherwise stated, all chemicals, nucleotides and drugs were obtained from Sigma, U.K.

Molecular Pharmacology Fast Forward. Published on January 6, 2011 as DOI: 10.1124/mol.110.070037
This article has not been copyedited and formatted. The final version may differ from this version.

RESULTS

Sequence analysis of BmP2X. The EST clone BEACR91 was found to contain a full length open reading frame (Submitted to GenBank as Accession Number: HQ333533) encoding 414 amino acids with homology to the human P2X1-7 receptor family ranging from 30.6% (P2X7) to 43.6% identity (P2X4). Prediction of membrane topology using TMPred (Hofmann and Stoffel, 1993) and TopPredII (Claros and von Heijne, 1994) programs suggests a typical P2X topology with intracellular carboxy and amino termini, two transmembrane domains and a large extracellular loop. Typical features of vertebrate P2X receptors such as 10 extracellular cysteine residues, a consensus protein kinase C phosphorylation site in the amino terminal domain, and positive and aromatic residues thought to be involved in ATP binding are also conserved in *Bm*P2X.

BmP2X is an ATP gated ion channel. ATP evoked large (~15 μA) inward currents at recombinant *Bm*P2X receptors expressed in *Xenopus* oocytes (Fig. 1A). These currents displayed unusually slow kinetics taking 4.5 ± 0.7 seconds to reach peak and 17.0 ± 2.4 seconds to decay by 10% during the continued presence of agonist (n = 24). Even after prolonged application of agonist (up to 6 minutes) currents did not decay by 50% making measurement of T.50% (time for current to decay by 50%) impractical due to changes in holding current required to clamp oocytes at -60 mV over prolonged periods of large membrane currents. Despite this low level of current desensitization during the continued presence of agonist, a marked run-down in current amplitude was observed between sequential applications of agonist with current amplitudes ~12% of their original amplitude after 8 sequential 40 second applications of 100 μM ATP 5 minutes apart (Fig. 1C). The decline in amplitude between the 2^{nd} and 8^{th} applications was best fit with a single exponential (τ = 8.2 ± 1.3 min, n = 24 oocytes). The first ATP application was omitted from this fit as oocytes did not have a prior five minute recovery period at this time point. ATP had an EC_{50} of 67.1 μM with a Hill slope of 1.5 ± 0.03 (Fig. 1D). Adenosine, ADP and UTP (tested at 1mM) did not evoke currents at *Bm*P2X. The general P2 receptor antagonist suramin inhibited ATP evoked *Bm*P2X currents with an IC_{50} of 4.8 μM (Fig. 1E). However, there was a suramin

Molecular Pharmacology Fast Forward. Published on January 6, 2011 as DOI: 10.1124/mol.110.070037
This article has not been copyedited and formatted. The final version may differ from this version.

resistant component to the *Bm*P2X current that persisted at the highest concentration of suramin tested (300 μM).

Wild-type BmP2X is not potentiated by ivermectin but the mutation M362L confers ivermectin sensitivity. The macrocyclic lactone ivermectin is a broad spectrum antiparasitic agent used in human and veterinary medicine and has previously been shown to potentiate ATP activated currents in human and rat P2X4 (Khakh et al., 1999; Priel and Silberberg, 2004), the *Sch*P2X receptor from the blood fluke *Schistosoma mansoni* (Agboh et al., 2004) and the *Hd*P2X receptor from the tardigrade *Hypsibius dujardini* (Bavan et al., 2009). Since ivermectin is an effective treatment against *Boophilus microplus* infestation in cattle (Cramer et al., 1988a; Cramer et al., 1988b), we were interested to determine whether *Bm*P2X currents were similarly affected by ivermectin. Wild-type *Bm*P2X receptors show a marked run-down in current amplitude between sequential ATP applications which may mask any subtle effects of ivermectin. We therefore normalized 100 μM ATP responses in the presence of either 3 or 10 μM ivermectin to ATP responses five minutes before and five minutes after the test application. Ivermectin however had no significant effect on ATP evoked currents at both concentrations tested (Fig. 2B and C). Ivermectin acts as an allosteric modulator of P2X4 by interacting with the transmembrane regions (Silberberg et al., 2007) and several predominantly nonpolar residues lying on the same side of their respective helices have been identified that when mutated to cysteine disrupt ivermectin sensitivity (Jelinkova et al., 2008). From alignment of P2X transmembrane sequences, the sequence motif (G(L/I)(G/A)LL) in TM2 is seen to be present only in those P2X channels known to be ivermectin sensitive (*Sm*P2X, *Hd*P2X, hP2X4 and rP2X4) (Fig. 2A). The first and last residues in this motif have previously been shown to be essential for ivermectin sensitivity (Jelinkova et al., 2008). Since the wild-type *Bm*P2X receptor differed from this motif by only one amino acid (M362), we mutated this residue to leucine and tested for ivermectin sensitivity. Ivermectin potentiated ATP evoked currents at the M362L mutant by ~40% at both 3 and 10 μM ($P < 0.01$) (Fig. 2 B and C). The M362L mutation had no effect on current run-down between sequential agonist application (data not shown) but was slightly less sensitive to ATP with an EC_{50} of 117.5 μM (Fig. 2D). The triazapentadiene compound amitraz is also widely used

Molecular Pharmacology Fast Forward. Published on January 6, 2011 as DOI: 10.1124/mol.110.070037
This article has not been copyedited and formatted. The final version may differ from this version.

to treat tick infestation in cattle and we therefore also tested the effects of this compound on *BmP2X*. Amitraz alone (100 μM) did not evoke membrane currents in *Xenopus* oocytes expressing *Bm*P2X receptors (data not shown). However, when amitraz was co-applied with 100 μM ATP, membrane currents were potentiated by 22.5 ± 8 % and 93.9 ± 31% at 1 and 100 μM amitraz respectively (Fig. 2F).

The contribution of the intracellular domains in determining desensitization properties of BmP2X and hdP2X receptors. The slow desensitization properties of ATP evoked currents in *Bm*P2X receptors are in marked contrast to the exceptionally fast desensitization displayed by the *Hd*P2X receptor previously cloned from the tardigrade species *Hypsibius dujardini* (Bavan et al., 2009). In order to assess the contribution of the intracellular domains in determining these markedly contrasting desensitization kinetics, a series of six chimeric channels were generated by exchanging intracellular N- and C-termini between *Bm*P2X and *Hd*P2X (Fig. 3). All six chimeras produced functional ATP-gated channels (Fig. 3). However, maximal current amplitudes were significantly lower than the respective wild-type channels with some chimeras (A,C and D) producing currents less than 100 nA (Table 3). Nevertheless, clear changes in desensitization properties were apparent and these were quantified using the parameters of 10-90% rise time, I_{20} (% peak current after 20 seconds ATP application) and T.10% (time taken for the current to decay by 10%). With the exception of chimera A, ATP was slightly more potent at chimeric channels when compared to their respective wild-type (Fig. 4C, Table 2). Marginal (< 5 fold) shifts in ATP potency were observed for all chimeras and in each case 1mM ATP produced a maximal response. Chimera A, consisting of *Bm*P2X with the C-terminus replaced with that of *Hd*P2X displayed a rise time (269 ± 14ms (n = 23)) ~3.5 times faster ($P < 0.01$) than wild-type *Bm*P2X (Table 3). Chimera A currents initially desensitized rapidly with a mean T.10% of 364 ± 37ms followed by a much slower rate of desensitization reflected in an I_{20} value of 34.8 ± 1.7%. Similarly, replacement of the C-terminus of *Hd*P2X with that of *Bm*P2X in chimera C also resulted in a change in current kinetics towards that of the C-terminal donor channel with rise time, I_{20} (Fig. 4A) and T_{10} (Fig. 4 B) values all significantly slower ($P < 0.01$) than *Hd*P2X and similar to those of *Bm*P2X (Table 3). Exchange of N-terminal domain regions in chimeras B and D also resulted in phenotypic changes in current kinetics towards those of the donor

Molecular Pharmacology Fast Forward. Published on January 6, 2011 as DOI: 10.1124/mol.110.070037
This article has not been copyedited and formatted. The final version may differ from this version.

channel with chimera B becoming faster than *Bm*P2X and chimera D becoming slower than *Hd*P2X (Table 3). Despite the very small (~22nA) current amplitude displayed by chimera D it was clear that, similar to chimera A, this channel also displayed an initial rapid phase of desensitization (T.10% = 61 ± 7 ms (n = 16)) followed by a slower rate of desensitization which resulted in an I_{20} value of 52.7 ± 3.5%. Given the large shifts in desensitization properties resulting from exchange of a single intracellular N- or C-terminal domains, it was perhaps unexpected that exchange of both intracellular termini together in chimeras E and F resulted in a less pronounced change when compared to the single domain swap chimeras. Nevertheless, chimera E displayed T.10% and I_{20} values that were significantly ($P < 0.01$) faster than wild-type *Bm*P2X and chimera F was significantly slower than wild-type *Hd*P2X (Table 3, Fig. 4A and B).

Replacement of the intracellular domains disrupts the marked current run-down displayed by BmP2X. In contrast to *Bm*P2X, which displays a marked run-down in current amplitude between repeated applications of agonist (Fig. 1 B and C), *Hd*P2X shows little run-down in current amplitude with a five minute recovery period between sequential applications of agonist (Fig. 5 B). We therefore investigated current run-down after 6 sequential applications of ATP, 5 minutes apart, in chimeras A-F in order to assess the potential roles of intracellular domains in determining these differing phenotypes. Similar to wild-type *Hd*P2X, a small decrease in current amplitude between first and second responses was observed in chimeras A,B,D,E and F (Fig. 5). Subsequent applications however produced stable responses and the amplitude of the 2nd response was not significantly different to the 6th response ($P > 0.05$) (Fig. 5 B). The amplitude of responses in chimera C similarly did not show run-down between sequential applications and current amplitudes increased slightly during the course of the 6 applications.

Truncation of the C-terminus increases the rate of BmP2X desensitization but does not prevent current run-down. Replacement of the C-terminal domain in the fast desensitizing *Hd*P2X channel with that of the slowly desensitizing *Bm*P2X (chimera C) was sufficient to convert *Hd*P2X into a slowly desensitizing channel with T.10% decay time, 10-90% rise time and I_{20} values not significantly different from *Bm*P2X (Table 3). This suggests that the C-terminal domain plays a prominent role in

Molecular Pharmacology Fast Forward. Published on January 6, 2011 as DOI: 10.1124/mol.110.070037
This article has not been copyedited and formatted. The final version may differ from this version.

determining the slow current desensitization properties of *Bm*P2X and in order to investigate this further we created a series of truncation mutations by introducing premature stop codons in the C-terminal domain of *Bm*P2X. As an initial screen, stop codons were introduced at positions 408, 400, 394 and 388. Truncation at the first 3 of these positions resulted in functional channels with peak amplitudes > 7 μA and 10-90% rise time, T.10% and I_{20} values significantly ($P < 0.01$) faster than the wild-type *Bm*P2X channel (Table 3, Fig. 6). The truncation Y388Δ however produced a non functional channel. Removal of just the six terminal amino acids from the C-terminal domain by the mutation E408Δ was sufficient to produce marked speeding in the desensitization properties of the channel (Fig. 6). We therefore generated a further four truncation mutants within this 6 amino acid region to assess which residues were required for the slow desensitization properties of the wild-type *Bm*P2X channel. Removal of the terminal serine residue in the mutation S414Δ resulted in no significant change in current kinetics with 10-90% rise times, T.10% and I_{20} values all similar to wild-type (Table 3, Fig. 6C and D). Truncation at position 413, removing the terminal arginine and serine residues, however did result in a speeding of current desensitization with, T.10% and I_{20} values significantly ($P < 0.01$) faster than wild-type. This speeding in desensitization was more pronounced when truncations were made further upstream at positions 412 and 410 resulting in channels with very similar properties to the truncation mutants K400Δ and E408Δ. Similar to wild-type, all functional truncation mutants displayed a run-down in peak current amplitude after sequential application of 1mM ATP with a 5 minute recovery period resulting in current amplitudes ~12% of their original values after 6 sequential applications (Fig. 6E).

Positive charge at position 413 is required for the slow desensitization of BmP2X. Truncations of the intracellular C-terminal domain identified the end of this region as being important in determining the slow desensitization properties of *Bm*P2X since truncations upstream of position 413 disrupted the slow desensitizing phenotype. We therefore mutated R413 to alanine, aspartic acid or lysine in order to determine whether charge at this position was an important factor and also mutated Y411 to alanine since this nearby residue partially met the criteria for a consensus tyrosine phosphorylation site. ATP evoked currents in the Y411A mutant were not significantly different to those of the wild-type

Molecular Pharmacology Fast Forward. Published on January 6, 2011 as DOI: 10.1124/mol.110.070037
This article has not been copyedited and formatted. The final version may differ from this version.

channel (Fig. 7, Table 3) indicating that potential phosphorylation at this position does not play a role in determining the slow desensitizing phenotype. However, mutation of arginine 413 to alanine, thereby neutralizing the positive charge at this position, resulted in a speeding of desensitization such that T.10% and I_{20} values were significantly ($P < 0.01$) faster than wild-type. Converting the positive charge at this position to a negative charge further increased the initial rate of desensitization with mutant R413D displaying a T.10% ~4 times faster than R413A and ~20 times faster than wild-type. The current remaining after 20 seconds ATP application (I_{20}) however was very similar between the R413A and R413D with both mutants displaying approximately half the current of the wild-type channel at this time point (Table 3). Maintaining the positive charge at position 413 by mutation to lysine (mutant R413K) resulted in a wild-type phenotype with 10-100% rise time, T.10% and I_{20} values not significantly different from *Bm*P2X (Fig. 7, Table 3) demonstrating that it is positive charge rather than the arginine *per se* at this position that determines the slow desensitization properties of *Bm*P2X. Run-down after sequential ATP applications was still apparent in R413 and Y411A mutants with each, similar to wild-type, displaying peak current amplitudes ~15% of their original values after 6 sequential responses (Fig. 7D). The mutants R413A and R413D however initially showed an increase in current amplitude between the first and second responses before run-down occurred at a rate similar to wild-type between the 3rd and 6th responses (Fig. 7D). Interestingly a similar phenomenon was also observed with the R413Δ truncation mutant (Fig. 6E).

Molecular Pharmacology Fast Forward. Published on January 6, 2011 as DOI: 10.1124/mol.110.070037
This article has not been copyedited and formatted. The final version may differ from this version.

DISCUSSION

Functional evidence that *Bm*P2X corresponds to an ATP gated channel establishes the existence of P2X receptors in the phylum Arthropoda. This is of significance regarding our understanding of the evolution of purinergic signaling since P2X receptors are absent in the fully sequenced genomes of several other arthropods such as *Anopheles gambiae*, *Drosophila* and *Apis mellifera* suggesting a selective loss of P2X receptors within this phylum has occurred in insects.

The ectoparasite *Boophilus microplus* represents a significant problem to livestock production in tropical and sub-tropical regions through direct detrimental effects of blood feeding and also by the transmission of disease (Young et al., 1988). Our initial interest in *Bm*P2X stemmed from the possibility that this channel could represent a target for the antiparasitic drug ivermectin. Whilst *Bm*P2X proved to be ivermectin insensitive (Fig. 2C), key residues within TM2 showed homology with ivermectin sensitive P2X receptors (Fig. 2A). One obvious difference was *Bm*P2X M362 which is a leucine in ivermectin sensitive P2X receptors. As a *Bm*P2X gene SNP could have resulted in this difference we generated the mutant M362L. Leucine at position 362 conferred ivermectin sensitivity in *Bm*P2X confirming previous studies (Jelinkova et al., 2008) highlighting the importance of this residue in ivermectin binding. However, the effect of ivermectin on *Bm*P2X M362L was relatively modest (~40% potentiation) casting doubt on whether a potential SNP at this position could be of relevance to the development of ivermectin resistance in *Boophilus microplus* (Perez-Cogollo et al., 2010). The ectoparasiticide amitraz is also widely used to treat tick infestation and is thought to act via parasite muscle octopamine receptors (Chen et al., 2007). Amitraz is typically applied to cattle at a concentration of 0.025% (~850 μM) (Eamens et al., 2001; Mekonnen, 2001). This concentration would be sufficient to affect *Bm*P2X function as 100 μM amitraz approximately doubled ATP evoked currents (Fig. 2F). It is therefore possible that *Bm*P2X potentiation is an additional target for the parasitacide action of amitraz, particularly in view of the fact that P2X receptors are known to play important roles in muscle contractility (Surprenant and North, 2009).

Molecular Pharmacology Fast Forward. Published on January 6, 2011 as DOI: 10.1124/mol.110.070037
This article has not been copyedited and formatted. The final version may differ from this version.

The extremely slow kinetics of *Bm*P2X led us to utilize this receptor as a model to probe mechanisms of desensitization. Chimeras produced by swapping N- and C-terminal domains between the fast desensitizing *Hd*P2X and slow desensitizing *Bm*P2X were used to investigate the importance of intracellular domains in determining current desensitization and run-down. Whilst interpretation of these chimeric studies is complicated by difficulties in distinguishing between effects caused by introduction of a new domain and those resulting from removal of the replaced domain, the overall pattern that emerged was that both N- and C-termini both play important roles in determining desensitization. However, the extent to which a particular domain exerts its effect depends upon the context in which it is placed. For example, considering the 2 chimeras that resulted in the most complete fast-to-slow or slow-to-fast phenotype reversal (chimeras B and C), the N-terminal domain of the fast desensitizing *Hd*P2X appears to exert a dominant fast desensitizing effect on the slow *Bm*P2X C-terminal domain (chimera B). However, when the slow *Bm*P2X C-terminal is placed in the context of the fast desensitizing *Hd*P2X (chimera C), it is the slow *Bm*P2X C-terminal that dominates over the fast *Hd*P2X N-terminal. A composite phenotype of fast and slow desensitizing components resulted when either the *Hd*P2X C-terminal was placed in the context of *Bm*P2X or the *Bm*P2X N-terminal was placed in the context of *Hd*P2X (chimeras A and D respectively). Taken together these finding suggest that whilst both terminal domains of both receptors can modulate desensitization, in *Hd*P2X it is the N-terminal domain that is most important for fast desensitization whereas in *Bm*P2X it is the C-terminal domain that is most important for slow desensitization. When both N- and C-termini were exchanged together, a similar slow-to-fast (chimera E) and fast-to-slow (chimera F) reversal was observed. However, the effects of double N- and C-terminal exchange were not as pronounced as those in single exchanges suggesting that in addition to potentially interacting with each other, the intracellular domains may also couple with other regions of the receptor, as has been proposed for P2X2 (He et al., 2002) and that these interactions are disrupted more by exchange of a single intracellular domain than by exchange of both domains together. Chimeras generated by exchange of transmembrane regions linked to N- or C-terminal domains between the fast desensitizing P2X1 (or P2X3) and the slow desensitizing P2X2 receptor previously demonstrated that transmembrane

Molecular Pharmacology Fast Forward. Published on January 6, 2011 as DOI: 10.1124/mol.110.070037
This article has not been copyedited and formatted. The final version may differ from this version.

domains play an important role in desensitization (Werner et al., 1996). The *Bm-HdP2X* chimeras utilized in this current study however involved exchange of only intracellular domains and therefore demonstrate that both these regions can modulate desensitization independently from their respective transmembrane sequence. This is also supported by the naturally occurring P2X2b (Brandle et al., 1997; Koshimizu et al., 1998; Simon et al., 1997) and mouse P2X2e (Koshimizu and Tsujimoto, 2006) splice variants, mutation of the protein kinase C site in the N-terminal domain (Boue-Grabot et al., 2000), mutation of a P2X4 C-terminal domain lysine residue (Fountain and North, 2006), and exchange of the C-terminal domains in P2X2 and P2X3 receptors (Paukert et al., 2001).

The intracellular C-terminal domains are highly variable in length between different P2X receptors and share little sequence similarity. The functional significance of this divergence is unclear but likely arises from the evolution of different regulatory mechanisms to control channel function. To further investigate the significance of the *Bm*P2X C-terminal domain in regulating slow desensitization, we first generated a series of truncation mutants (Fig. 6). Similar to zebrafish P2X4 (Kawate et al., 2009), *Bm*P2X channel function was quite tolerant to C-terminal truncation with all truncations up to and including E394 producing functional channels (Fig. 6). This is in contrast to human P2X4 where deletion of the terminal 15 amino acids prevented function (Fountain and North, 2006). No ATP evoked currents were observed in the Y388Δ truncation suggesting that the minimal C-terminal domain length required for *Bm*P2X function lies between residues 388 and 394. All functional *Bm*P2X truncations before the terminal serine at position 414 resulted in a speeding in the rate of desensitization (Fig. 6B), suggesting that the very end of the C-terminal domain is important in determining the slow desensitization properties of *Bm*P2X. Indeed, disruption of the positive charge at the penultimate residue (R413) in the mutants R413A and R413D significantly increased the speed of channel desensitization (Fig. 7A). The fact that substitution for lysine at this same position (R413K) resulted in a wild-type phenotype demonstrates that it is the positive charge at this position that is crucial for slow desensitization rather than arginine *per se*. Amongst human, rat and mouse P2X1-7 and the known invertebrate P2X receptors, *Bm*P2X is the only channel with an arginine at the penultimate position. A positively charged C-terminal lysine residue has also been shown to be

Molecular Pharmacology Fast Forward. Published on January 6, 2011 as DOI: 10.1124/mol.110.070037
This article has not been copyedited and formatted. The final version may differ from this version.

important for slow desensitization in P2X4, however, in this case it is the amino group rather than the positive charge that is critical (Fountain and North, 2006).

In addition to desensitization during the continued presence of agonist, *Bm*P2X responses also displayed a marked run-down in current amplitude between sequential applications of agonist. The lack of run-down in the *Bm*P2X based chimeras A,B and E suggests that, in addition to regulating desensitization during the continued presence of agonist, intracellular domains may also play a role in the mechanism of run-down between sequential responses, possibly by influencing the rate of receptor internalization (Dutton et al., 2000) and trafficking (Bobanovic et al., 2002). However, the *Bm*P2X N- or C-termini when added to the *Hd*P2X core did not confer run-down suggesting that the intracellular domains are not the sole determinants. Furthermore, chimeric channels generally had smaller current amplitudes than wild-type channels making direct comparison of run-down difficult. C-terminal truncations (Fig. 6E) and R413 point mutants (Fig 7. D) did display peak current amplitudes that were comparable to wild-type *Bm*P2X (Table 3). In these mutant channels run-down and desensitization appeared to be independent processes since a marked increase in desensitization was not accompanied by a significant alteration in the rate of run-down after 6 sequential ATP applications. It was however interesting that truncation R413Δ and the point mutants R413A and R413D (but not R413K) initially showed an increase in current amplitude between first and second responses before run-down occurred at a rate similar to wild-type (Figs. 6E and 7D). The reason for this is unclear but given that R413 plays a key role in desensitization, it could suggest that whilst desensitization and run-down are largely governed by distinct mechanisms, positive charge at position 413 could also have a minor influence on run-down.

In summary, this study presents a new member of the P2X receptor family, *Bm*P2X and identifies a novel example by which P2X desensitization is regulated by positive charge at the end of the C-terminus. *Bm*P2X may also be of importance to the cattle industry either as a potential target for new antiparasitic agents or as an epitope for vaccines against tick infestation.

Molecular Pharmacology Fast Forward. Published on January 6, 2011 as DOI: 10.1124/mol.110.070037
This article has not been copyedited and formatted. The final version may differ from this version.

ACKNOWLEDGEMENTS

We are grateful to Amina Bassou for technical assistance in the generation of truncation mutants and to Manijeh Maleki-Dizaji for the preparation of *Xenopus* oocytes.

Molecular Pharmacology Fast Forward. Published on January 6, 2011 as DOI: 10.1124/mol.110.070037
This article has not been copyedited and formatted. The final version may differ from this version.

AUTHOR CONTRIBUTIONS

Participated in research design: Ennion

Conducted experiments: Bavan, Farmer, Singh, Guerrero, Ennion

Performed data analysis: Bavan, Farmer, Singh, Ennion

Wrote or contributed to the writing of the manuscript: Straub, Guerrero, Ennion

REFERENCES

Agboh KC, Webb TE, Evans RJ and Ennion SJ (2004) Functional characterization of a P2X receptor from Schistosoma mansoni. *J Biol Chem* **279**(40):41650-41657.

Barrera NP, Ormond SJ, Henderson RM, Murrell-Lagnado RD and Edwardson JM (2005) Atomic force microscopy imaging demonstrates that P2X2 receptors are trimers but that P2X6 receptor subunits do not oligomerize. *J Biol Chem* **280**(11):10759-10765.

Bavan S, Straub VA, Blaxter ML and Ennion SJ (2009) A P2X receptor from the tardigrade species Hypsibius dujardini with fast kinetics and sensitivity to zinc and copper. *BMC Evol Biol* **9**:17.

Bobanovic LK, Royle SJ and Murrell-Lagnado RD (2002) P2X receptor trafficking in neurons is subunit specific. *J Neurosci* **22**(12):4814-4824.

Boue-Grabot E, Archambault V and Seguela P (2000) A protein kinase C site highly conserved in P2X subunits controls the desensitization kinetics of P2X(2) ATP-gated channels. *J Biol Chem* **275**(14):10190-10195.

Brandle U, Spielmanns P, Osteroth R, Sim J, Surprenant A, Buell G, Ruppersberg JP, Plinkert PK, Zenner HP and Glowatzki E (1997) Desensitization of the P2X(2) receptor controlled by alternative splicing. *FEBS Lett* **404**(2-3):294-298.

Browne LE, Jiang LH and North RA (2010) New structure enlivens interest in P2X receptors. *Trends Pharmacol Sci* **31**(5):229-237.

Chen AC, He H and Davey RB (2007) Mutations in a putative octopamine receptor gene in amitraz-resistant cattle ticks. *Vet Parasitol* **148**(3-4):379-383.

Claros MG and von Heijne G (1994) TopPred II: an improved software for membrane protein structure predictions. *Comput Appl Biosci* **10**(6):685-686.

Clyne JD, Wang LF and Hume RI (2002) Mutational analysis of the conserved cysteines of the rat P2X2 purinoceptor. *J Neurosci* **22**(10):3873-3880.

Cramer LG, Bridi AA, Amaral NK and Gross SJ (1988a) Persistent activity of injectable ivermectin in the control of the cattle tick Boophilus microplus. *Vet Rec* **122**(25):611-612.

Cramer LG, Carvalho LA, Bridi AA, Amaral NK and Barrick RA (1988b) Efficacy of topically applied ivermectin against Boophilus microplus (Canestrini, 1887) in cattle. *Vet Parasitol* **29**(4):341-349.

Dutton JL, Poronnik P, Li GH, Holding CA, Worthington RA, Vandenberg RJ, Cook DI, Barden JA and Bennett MR (2000) P2X(1) receptor membrane redistribution and down-regulation visualized by using receptor-coupled green fluorescent protein chimeras. *Neuropharmacology* **39**(11):2054-2066.

Eamens G, Spence S and Turner M (2001) Survival of Mycobacterium avium subsp paratuberculosis in amitraz cattle dip fluid. *Aust Vet J* **79**(10):703-706.

Ennion S, Hagan S and Evans RJ (2000) The role of positively charged amino acids in ATP recognition by human P2X(1) receptors. *J Biol Chem* **275**(38):29361-29367.

Ennion SJ and Evans RJ (2002a) Conserved cysteine residues in the extracellular loop of the human P2X(1) receptor form disulfide bonds and are involved in receptor trafficking to the cell surface. *Mol Pharmacol* **61**(2):303-311.

Ennion SJ and Evans RJ (2002b) P2X(1) receptor subunit contribution to gating revealed by a dominant negative PKC mutant. *Biochem Biophys Res Commun* **291**(3):611-616.

Fountain SJ and North RA (2006) A C-terminal lysine that controls human P2X4 receptor desensitization. *J Biol Chem* **281**(22):15044-15049.

Guerrero FD, Miller RJ, Rousseau ME, Sunkara S, Quackenbush J, Lee Y and Nene V (2005) BmiGI: a database of cDNAs expressed in Boophilus microplus, the tropical/southern cattle tick. *Insect Biochem Mol Biol* **35**(6):585-595.

He ML, Koshimizu TA, Tomic M and Stojilkovic SS (2002) Purinergic P2X(2) receptor desensitization depends on coupling between ectodomain and C-terminal domain. *Mol Pharmacol* **62**(5):1187-1197.

Hofmann K and Stoffel W (1993) TMbase - A database of membrane spanning proteins segments. *Biol Chem* **374**:166.

Jelinkova I, Vavra V, Jindrichova M, Obsil T, Zemkova HW, Zemkova H and Stojilkovic SS (2008) Identification of P2X(4) receptor transmembrane residues contributing to channel gating and interaction with ivermectin. *Pflugers Arch* **456**(5):939-950.

Kawate T, Michel JC, Birdsong WT and Gouaux E (2009) Crystal structure of the ATP-gated P2X(4) ion channel in the closed state. *Nature* **460**(7255):592-598.

Khakh BS, Proctor WR, Dunwiddie TV, Labarca C and Lester HA (1999) Allosteric control of gating and kinetics at P2X(4) receptor channels. *J Neurosci* **19**(17):7289-7299.

Koshimizu T, Tomic M, Koshimizu M and Stojilkovic SS (1998) Identification of amino acid residues contributing to desensitization of the P2X2 receptor channel. *J Biol Chem* **273**(21):12853-12857.

Koshimizu TA and Tsujimoto G (2006) Functional role of spliced cytoplasmic tails in P2X2-receptor-mediated cellular signaling. *J Pharmacol Sci* **101**(4):261-266.

Mekonnen S (2001) In vivo evaluation of amitraz against ticks under field conditions in Ethiopia. *J S Afr Vet Assoc* **72**(1):44-45.

Nicke A, Baumert HG, Rettinger J, Eichele A, Lambrecht G, Mutschler E and Schmalzing G (1998) P2X1 and P2X3 receptors form stable trimers: a novel structural motif of ligand-gated ion channels. *EMBO J* **17**(11):3016-3028.

Paukert M, Osteroth R, Geisler HS, Brandle U, Glowatzki E, Ruppersberg JP and Grunder S (2001) Inflammatory mediators potentiate ATP-gated channels through the P2X(3) subunit. *J Biol Chem* **276**(24):21077-21082.

Perez-Cogollo LC, Rodriguez-Vivas RI, Ramirez-Cruz GT and Rosado-Aguilar JA (2010) Survey of Rhipicephalus microplus resistance to ivermectin at cattle farms with history of macrocyclic lactones use in Yucatan, Mexico. *Vet Parasitol* **172**(1-2):109-113.

Priel A and Silberberg SD (2004) Mechanism of ivermectin facilitation of human P2X4 receptor channels. *J Gen Physiol* **123**(3):281-293.

Roberts JA, Vial C, Digby HR, Agboh KC, Wen H, Atterbury-Thomas A and Evans RJ (2006) Molecular properties of P2X receptors. *Pflugers Arch* **452**(5):486-500.

Silberberg SD, Li M and Swartz KJ (2007) Ivermectin Interaction with transmembrane helices reveals widespread rearrangements during opening of P2X receptor channels. *Neuron* **54**(2):263-274.

Simon J, Kidd EJ, Smith FM, Chessell IP, Murrell-Lagnado R, Humphrey PP and Barnard EA (1997) Localization and functional expression of splice variants of the P2X2 receptor. *Mol Pharmacol* **52**(2):237-248.

Stojilkovic SS, Tomic M, He ML, Yan Z, Koshimizu TA and Zemkova H (2005) Molecular dissection of purinergic P2X receptor channels. *Ann N Y Acad Sci* **1048**:116-130.

Surprenant A and North RA (2009) Signaling at purinergic P2X receptors. *Annu Rev Physiol* **71**:333-359.

Werner P, Seward EP, Buell GN and North RA (1996) Domains of P2X receptors involved in desensitization. *Proc Natl Acad Sci U S A* **93**(26):15485-15490.

Young AS, Groocock CM and Kariuki DP (1988) Integrated control of ticks and tick-borne diseases of cattle in Africa. *Parasitology* **96 (Pt 2)**:403-432.

Young MT (2009) P2X receptors: dawn of the post-structure era. *Trends Biochem Sci* **35**(2):83-90.

Zemkova H, He ML, Koshimizu TA and Stojilkovic SS (2004) Identification of ectodomain regions contributing to gating, deactivation, and resensitization of purinergic P2X receptors. *J Neurosci* **24**(31):6968-6978.

FOOTNOTES

This work was supported by the Wellcome Trust [Grant WT081601MA] and a Biotechnology and Biological Sciences Research Council Studentship to S.B.

Reprint requests to: Dr Steven J. Ennion, Department of Cell Physiology and Pharmacology, University of Leicester, Leicester, United Kingdom, LE19HN. Email: se15@le.ac.uk

Molecular Pharmacology Fast Forward. Published on January 6, 2011 as DOI: 10.1124/mol.110.070037
This article has not been copyedited and formatted. The final version may differ from this version.

FIGURE LEGENDS

Figure 1. *Bm*P2X is a slowly desensitizing ATP gated ion channel. Membrane currents were recorded by two-electrode voltage clamp in *Xenopus* oocytes expressing *Bm*P2X receptors. A) Example current traces in response to a 40 second application (solid black bar) of 1 mM ATP (left) or 1mM ADP (right). B) Consecutive responses from the same oocyte demonstrating a marked run down in current amplitude with sequential 40 second applications of 100 μM ATP and a five minute recovery period between the end of one application and the start of the next. C) Mean data expressed as % peak current amplitude of the first response for consecutive ATP applications as described in B (n = 24 oocytes). Dotted line shows a single exponential fit (excluding time point zero), τ = 8.2 minutes. D) Concentration response curve for ATP in *Bm*P2X expressing oocytes. Mean currents (± S.E.M) were normalized to responses given by 100 μM ATP, EC_{50} = 67.1 μM (n = 7 oocytes). E) Inhibition curve for mean responses to 100 μM ATP in the presence of different concentrations of suramin (IC_{50} = 4.8 μM) (n = 7).

Figure 2. The mutation M362L confers ivermectin sensitivity in *BM*P2X. A) Amino acid alignment of the region surrounding transmembrane domain 2 (TM2) in *Bm*P2X, *Schistosoma mansoni* P2X (*Sm*P2X) (Agboh et al., 2004), *Hypsibius dujardini* P2X (*Hd*P2X) (Bavan et al., 2009), rat P2X4 and human P2X1-7 receptors. Ivermectin sensitive receptors are highlighted by gray background. A TM2 motif (G(L/I)(G/A)LL) present only in those receptors sensitive to ivermectin is highlighted in bold. B) Example two-electrode voltage clamp recordings from wild-type and M362L *Bm*P2X expressing *Xenopus* oocytes. ATP (100 μM) evoked currents were recorded from the same cell in the presence and absence of 3 μM ivermectin (+IVM) (applications indicated by bars). A five minute recovery period was allowed between applications and ivermectin was bath perfused in the five minutes preceding the second recording as well as being present in the ATP application. C) Mean data for ATP (100 μM) responses in the presence and absence of ivermectin (3 or 10 μM) as described in B. Ivermectin responses were normalized to the mean of the bracketing ATP responses 5 minutes prior and 5 minutes after the

Molecular Pharmacology Fast Forward. Published on January 6, 2011 as DOI: 10.1124/mol.110.070037
This article has not been copyedited and formatted. The final version may differ from this version.

ivermectin response. ** denotes $P < 0.01$and ns $P > 0.05$ in comparison to the wild-type control response (n = 10-15). D) ATP concentration response curve for M362L (n = 8). The wild-type *Bm*P2X curve (gray) is also shown for comparison. E) Example wild-type *Bm*P2X current traces to sequential applications (5 minutes apart) of ATP (100 μM) in the presence and absence of 100 μM amitraz (+AMZ). F) Mean data (n = 12-15) for ATP (100 μM) responses in the presence and absence of amitraz (1 or 10 μM) (protocol as described in B).

Figure 3. Changes in desensitization properties after exchange of intracellular domains in chimeric channels. Example membrane currents in response to a 30 second application of 1mM ATP (black bars) are shown for wild-type and intracellular domain chimeras between *Bm*P2X (gray) and *Hd*P2X (white) channels.

Figure 4. Quantification of current desensitization in *Xenopus* oocytes expressing wild-type and chimeric *Bm-Hd*P2X channels. A) I_{20} (% peak current amplitude remaining after 20 seconds ATP application) values for membrane currents in response to a 30 second application of 1mM ATP (n = 15-25). B) T.10% (time taken for the current to decay by 10% from peak amplitude) values for same traces as in A) (note log scale of y axis). ** and ‡‡ denote a significant difference ($P < 0.01$) to wild-type *Bm*P2X and *Hd*P2X respectively (* = $P < 0.05$). C) Concentration response curves for wild-type and chimeric channels (see table 2).

Figure 5. Replacement of intracellular domains in *Bm*P2X chimeras prevents the marked current run down observed in WT *Bm*P2X. A) Example consecutive responses to a 30 second application of 1mM ATP (solid bars) with a five minute recovery period between applications in *Xenopus* oocytes expressing chimeras consisting of a *Bm*P2X core (chimeras A,B and E). The marked run down in current amplitude to sequential ATP applications displayed by wild-type *Bm*P2X is abolished in these chimeras. B) Mean

Molecular Pharmacology Fast Forward. Published on January 6, 2011 as DOI: 10.1124/mol.110.070037
This article has not been copyedited and formatted. The final version may differ from this version.

peak current amplitudes to sequential application of ATP (1mM, 5 minutes apart) in wild-type *Bm*P2X and *Hd*P2X (dashed lines) and chimeric channels (n = 5-7).

Figure 6. Truncation of the *Bm*P2X C-terminal tail increases the rate of current desensitization. A) *Bm*P2X C-terminal domain sequence indicating positions of truncation mutants (arrows). Predicted TM2 domain sequence is highlighted in gray. B) Example current traces to a 40 second application of 1mM ATP (black bar) recorded form *Xenopus* oocytes expressing *Bm*P2X C-terminal truncation mutants. C) and D) Mean I_{20} and T.10% values for truncation mutants (n = 12-18). ** denotes a significant difference to wild-type ($P < 0.01$). NF in the case of Y388Δ denotes a non functional channel. E) Mean peak current amplitudes to sequential application of ATP (1mM, 5 minutes apart) in wild-type (WT) *Bm*P2X (dashed line) and truncation mutants (n = 7-9).

Figure 7. Mutation of arginine 413 demonstrates that positive charge in this position is essential for the slow desensitizing phenotype of wild-type *Bm*P2X. A) Example current traces recorded from *Xenopus* oocytes expressing Y411 and R413 mutant *Bm*P2X channels. Removal of positive charge in mutants R413A and R413D speeds the rate of current desensitization whereas slow desensitization is restored in mutant R413K. B) and C) Mean I_{20} and T.10% values for truncation mutants (n = 8-15). ** denotes a significant difference to wild-type ($P < 0.01$). D) Mean peak current amplitudes to sequential application of ATP (1mM, 5 minutes apart) in wild-type (WT) *Bm*P2X (dashed line) and point mutants (n = 7-8).

Molecular Pharmacology Fast Forward. Published on January 6, 2011 as DOI: 10.1124/mol.110.070037
This article has not been copyedited and formatted. The final version may differ from this version.

TABLES

Table 1

Oligonucleotide primers

		Forward primer (5'-3')	Reverse primer (5'-3')	Region
1	*Bm*P2X	GCCGCCACCATGGGCTTGAACTGCG	GCATACACTTGAGTGCTCG	1-414
2	*Bm*P2X N-TM2	GCCGCCACCATGGGCTTGAAC	AA**CTCTTC**ACAGCAGGCAGTTAAGAACAACAAG	1-378
3	*Hd*P2X N-TM2	GCCGCCACCATGACGAATTTCACTAATACG	AA**CTCTTC**ACTTCAGGAAGTCCGTTAAAAAGTC	1-371
4	*Bm*P2X TM1-C	AA**CTCTTC**ACGTATCGGCGTGCTCAACAGGCTC	AGTGCTCGTTAGCATGCTCC	28-414
5	*Hd*P2X TM1-C	AA**CTCTTC**AAAGTTGGGCGCCATCAATCGGAC	GGAGTTTTGGTAGCGCACAG	40-480
6	*Bm*P2X N	Forward primer 2 above	AA**CTCTTC**ACTTTTTGTTGCCGATGTGGAC	1-28
7	*Hd*P2X N	Forward primer 3 above	AA**CTCTTC**AACGAGTGCTGTAGACCTTGAC	1-40
8	*Bm*P2X C	AA**CTCTTC**AAAGCGTCGTGATCTGTACAAG	Reverse primer 4 above	378-414
9	*Hd*P2X C	AACTCTTCAAAGCGTCGTGATCTGTACAAG	Reverse primer 5 above	371-480

Primer pair 1: Amplification of the *Bm*P2X wild-type sequence to introduce a mammalian Kozak sequence. Primer pairs 2-9: *Bm*P2X-*Hd*P2X chimera generation, N and C signify amino and carboxy termini respectively, TM transmembrane domain. Region refers to the amino acid positions encoded in the resulting PCR product. *EarI* endonuclease recognition sites incorporated into primers are in bold.

Molecular Pharmacology Fast Forward. Published on January 6, 2011 as DOI: 10.1124/mol.110.070037
This article has not been copyedited and formatted. The final version may differ from this version.

Table 2

ATP Concentration response data

Channel	EC_{50} (μM)	pEC_{50}	Hill Slope
WT *Bm*P2X	67.1	4.17 ± 0.03	1.5 ± 0.03
*Bm*P2X M362L	117.5	3.93 ± 0.03	2.7 ± 0.03
*Hd*P2X	25.5	4.59 ± 0.04	1.2 ± 0.01
Chimera A	100.2	4.00 ± 0.06	1.0 ± 0.12
Chimera B	34.8	4.46 ± 0.07	0.9 ± 0.11
Chimera C	5.2	5.29 ± 0.05	0.7 ± 0.06
Chimera D	12.1	4.92 ± 0.06	0.5 ± 0.04
Chimera E	7.2	5.14 ± 0.06	1.1 ± 0.13
Chimera F	6.9	5.16 ± 0.04	0.8 ± 0.05

Molecular Pharmacology Fast Forward. Published on January 6, 2011 as DOI: 10.1124/mol.110.070037
This article has not been copyedited and formatted. The final version may differ from this version.

Table 3

Properties of ATP evoked currents in wild-type, mutant and chimeric P2X channels

Channel	Peak current (nA)	10-90% Rise time (ms)	100-90% Decay time (ms) (T.10%)	% Peak current after 20 s (I_{20})
WT *Bm*P2X	-14677 ± 882 ††	951 ± 129 ††	17016 ± 2420 ††	86.6 ± 1.7 ††
WT *Hd*P2X	-1808 ± 141 **	65 ± 2 **	46 ± 3 **	0.1 ± 0.08 **
Chimera A	-77 ± 6 **††	269 ± 14 **††	364 ± 37 **††	34.8 ± 1.7 **††
Chimera B	-1282 ± 165 **	281 ± 8 **††	237 ± 10 **††	2.9 ± 0.2 **††
Chimera C	-63 ± 4 **††	1730 ± 192 ††	10020 ± 1391 ††	82.4 ± 1.5 ††
Chimera D	-22 ± 1 **††	195 ± 12 **	61 ± 7 **	52.7 ± 3.5 **††
Chimera E	-5441 ± 538	1072 ± 70 ††	1388 ± 92 **††	10.6 ± 1.1 **††
Chimera F	-196 ± 12 **††	482 ± 39 ††	1882 ± 249 **††	54.7 ± 1.7 *††
S414Δ	-14056 ± 628 ††	1515 ± 230 ††	16244 ± 1374 ††	88.6 ± 1.6 ††
R413Δ	-11720 ± 883 ††	588 ± 75 ††	6469 ± 766 **††	68.3 ± 3.3 **††
L412Δ	-8600 ± 1043 **††	454 ± 39 ††	700 ± 41 **††	5.1 ± 1.1 **††
F410Δ	-8670 ± 857 **††	491 ± 31 ††	764 ± 41 **††	8.4 ± 1.1 **††
E408Δ	-15812 ± 1152 ††	358 ± 23 **††	1118 ± 113 **††	13.2 ± 1.7 **††
K400Δ	-7078 ± 864 **††	276 ± 35 **††	620 ± 77 **††	9.8 ± 1.7 **††
E394Δ	-14263 ± 1194 ††	328 ± 14 **††	1337 ± 140 **††	26.1 ± 2.6 **††
Y388Δ	NF	NF	NF	NF
Y411A	-14379 ± 580 ††	731 ± 113 ††	16207 ± 4615 ††	79.0 ± 3.8 ††
R413K	-11640 ± 1168 ††	1500 ± 313 ††	15455 ± 3934 ††	84.5 ± 3.0 ††
R413A	-7805 ± 1476 **††	624 ± 91 ††	2964 ± 396 **††	43.4 ± 5.7 **††
R413D	-7435 ± 871 **††	275 ± 24 **††	758 ± 50 **††	40.0 ± 3.2 **††

Values are means ± S.E.M . * ($P < 0.05$) and **($P < 0.01$) denote a significant difference to wild-type *Bm*P2X. † ($P < 0.05$) and †† ($P < 0.01$) denote a significant difference to wild-type *Hd*P2X. Y388Δ was non-functional (NF). n ≥ 15 for each channel.

Figure 1

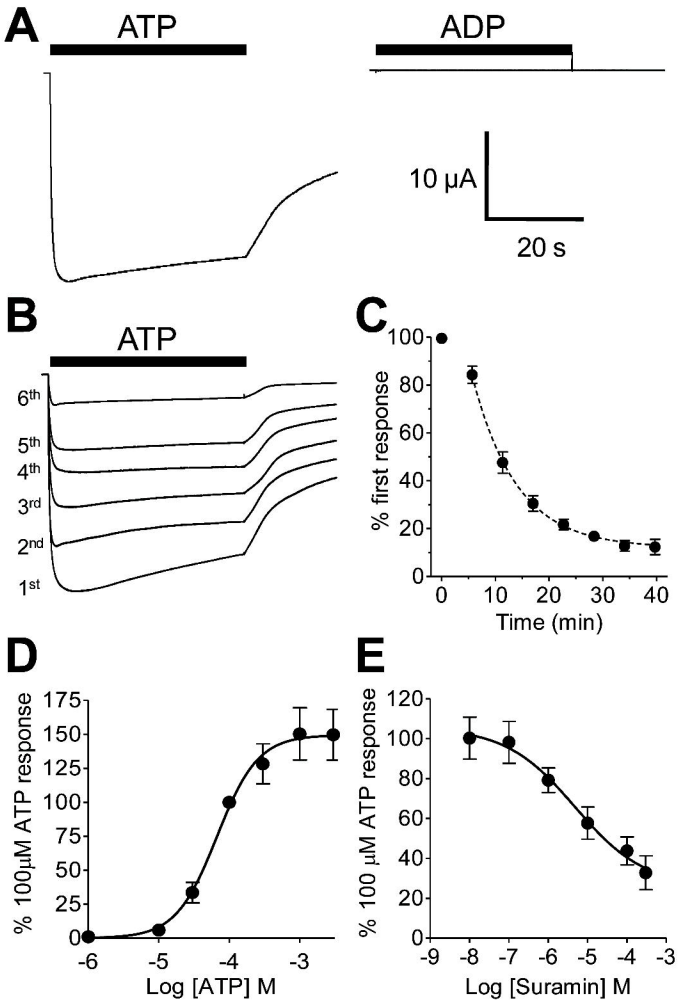
A
ATP
ADP
10 µA
20 s
B
ATP
6th
5th
4th
3rd
2nd
1st
C
% first response
Time (min)
D
% 100µM ATP response
Log [ATP] M
E
% 100 µM ATP response
Log [Suramin] M

Figure 2

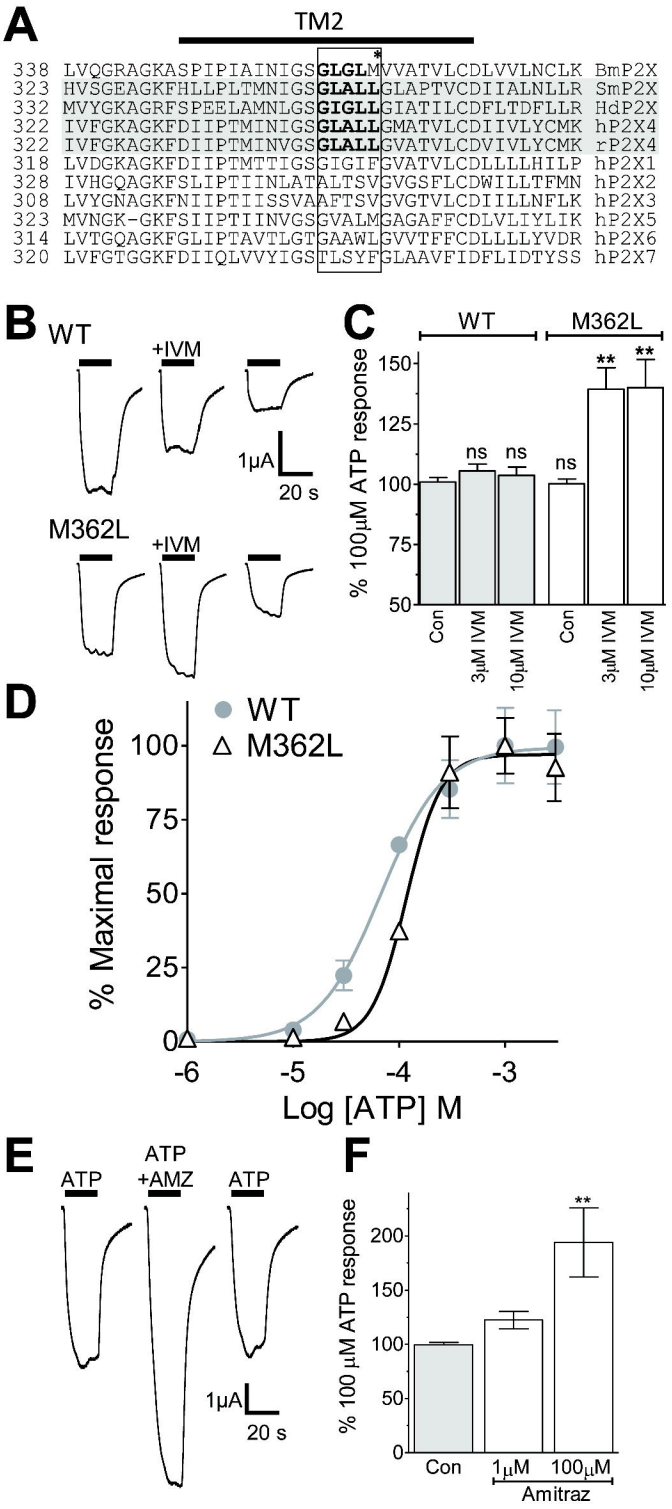
A
TM2
338 LVQGRAGKASPIPIAINIGSGLGLMVVATVLCDLVVLNCLK BmP2X
323 HVSGEAGKFHLLPLTMNIGSGLALLGLAPTVCDIIALNLLR SmP2X
332 MVYGKAGRFSPEELAMNLGSGIGLLGIATILCDFLTDFLLR HdP2X
322 IVFGKAGKFDIIPTMINIGSGLALLGMATVLCDIIVLYCMK hP2X4
322 IVFGKAGKFDIIPTMINVGSGLALLGVATVLCDVIVLYCMK rP2X4
318 LVDGKAGKFDIIPTMTTIGSGIGIFGVATVLCDLLLLHILP hP2X1
328 IVHGQAGKFSLIPTIINLATALTSVGVGSFLCDWILLTFMN hP2X2
308 LVYGNAGKFNIIPTIISSVAAFTSVGVGTVLCDIILLNFLK hP2X3
323 MVNGK-GKFSIIPTIINVGSGVALMGAGAFFCDLVLIYLIK hP2X5
314 LVTGQAGKFGLIPTAVTLGTGAAWLGVVTFFCDLLLLYVDR hP2X6
320 LVFGTGGKFDIIQLVVYIGSTLSYFGLAAVFIDFLIDTYSS hP2X7
B
WT
+IVM
1μA
20 s
M362L
+IVM
C
WT
M362L
% 100μM ATP response
150
125
100
75
50
ns
ns
ns
**
**
Con
3μM IVM
10μM IVM
Con
3μM IVM
10μM IVM
D
WT
M362L
% Maximal response
100
75
50
25
0
-6
-5
-4
-3
Log [ATP] M
E
ATP
ATP +AMZ
ATP
1μA
20 s
F
% 100 μM ATP response
200
150
100
50
0
**
Con
1μM
100μM
Amitraz

Figure 3

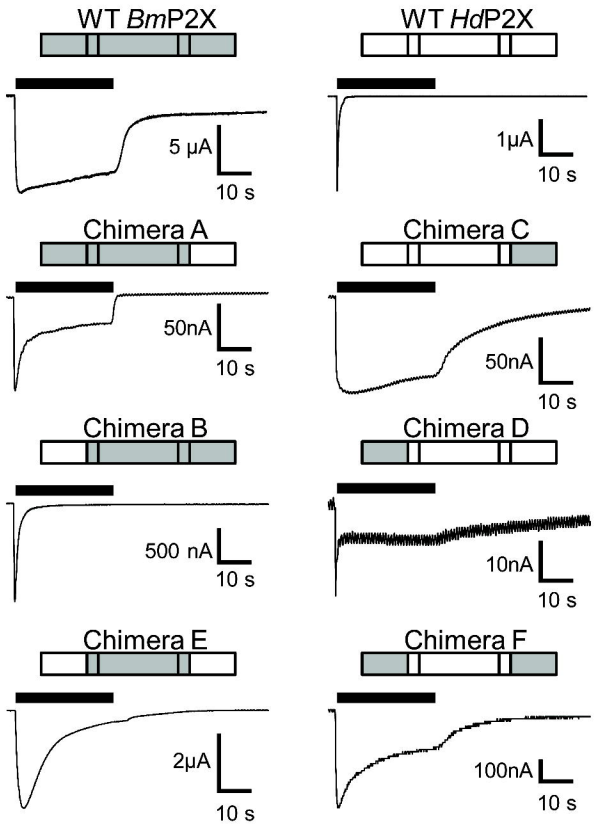
WT *Bm*P2X
5 µA
10 s
WT *Hd*P2X
1µA
10 s
Chimera A
50nA
10 s
Chimera C
50nA
10 s
Chimera B
500 nA
10 s
Chimera D
10nA
10 s
Chimera E
2µA
10 s
Chimera F
100nA
10 s

Figure 4

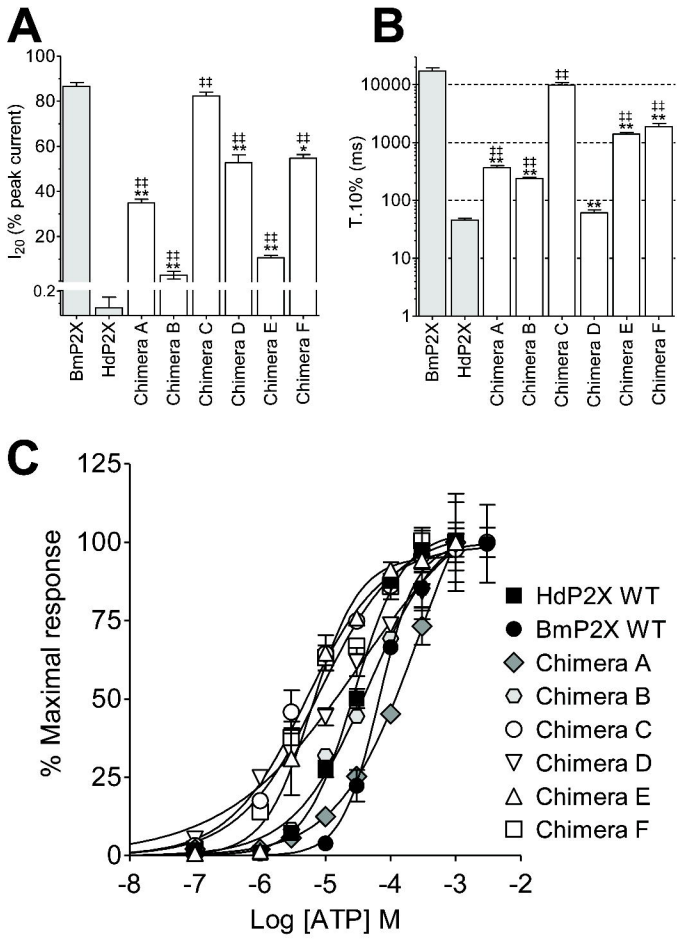
A
B
C
I_{20} (% peak current)
T.10% (ms)
BmP2X
HdP2X
Chimera A
Chimera B
Chimera C
Chimera D
Chimera E
Chimera F
% Maximal response
Log [ATP] M
HdP2X WT
BmP2X WT

Figure 5

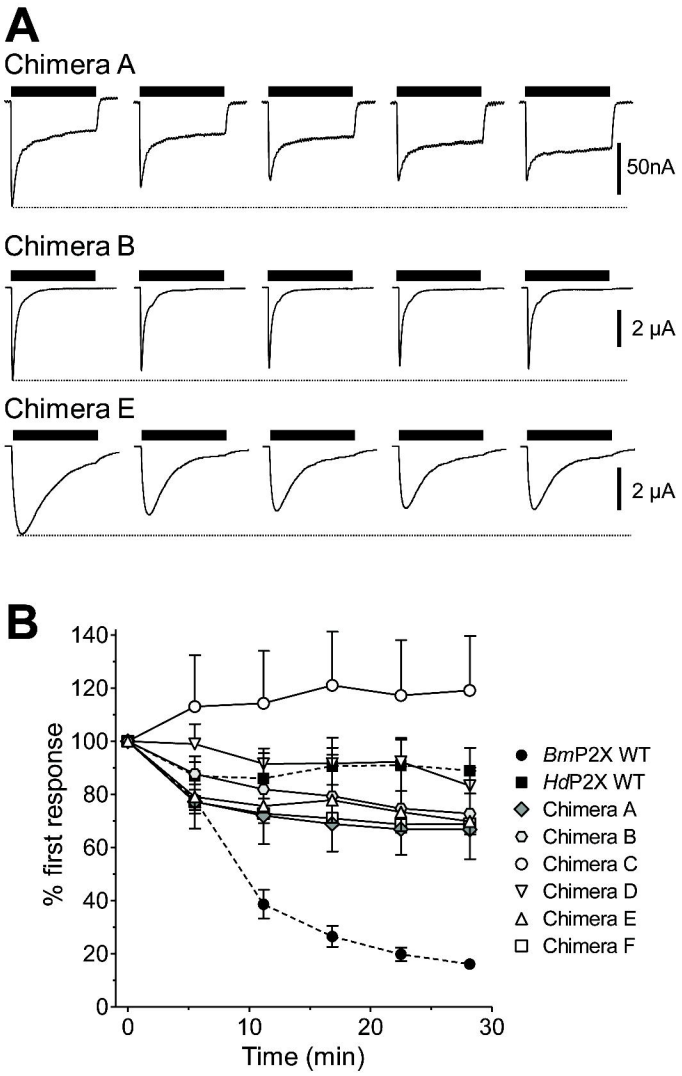
A
Chimera A
50nA
Chimera B
2 µA
Chimera E
2 µA
B
% first response
Time (min)
0
20
40
60
80
100
120
140
0
10
20
30
BmP2X WT
HdP2X WT
Chimera A
Chimera B
Chimera C
Chimera D
Chimera E
Chimera F

Figure 6

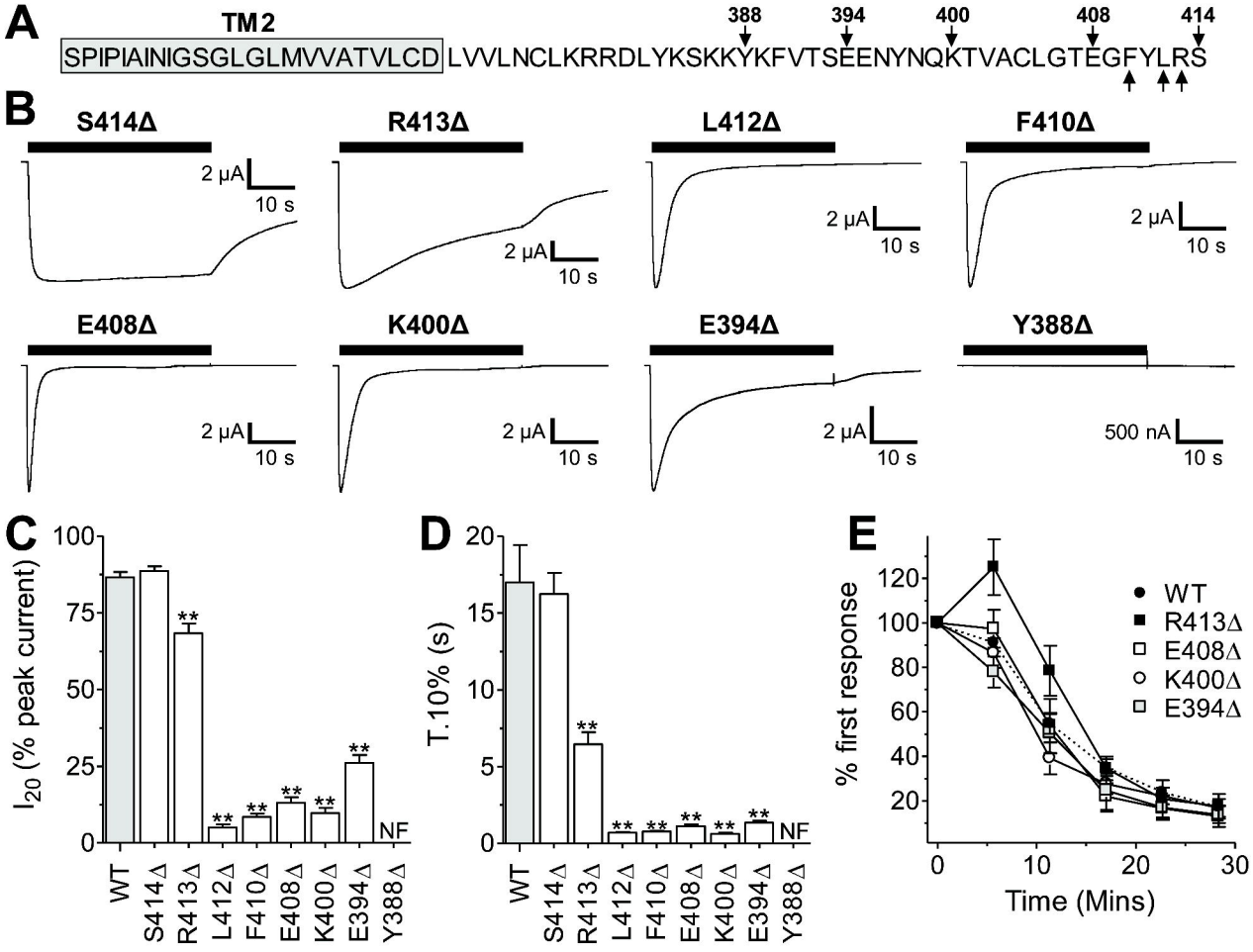
A
TM2
388
394
400
408
414
SPIPIAINIGSGLGLMVVATVLCD LVVLNCLKRRDLYKSKKYKFVTSEENYNQKTVACLGTEGFYLRS
B
S414Δ
R413Δ
L412Δ
F410Δ
E408Δ
K400Δ
E394Δ
Y388Δ
2 μA
10 s
500 nA
C
I20 (% peak current)
D
T.10% (s)
NF
WT
S414Δ
R413Δ
L412Δ
F410Δ
E408Δ
K400Δ
E394Δ
Y388Δ
E
% first response
Time (Mins)
WT
R413Δ
E408Δ
K400Δ
E394Δ

Figure 7

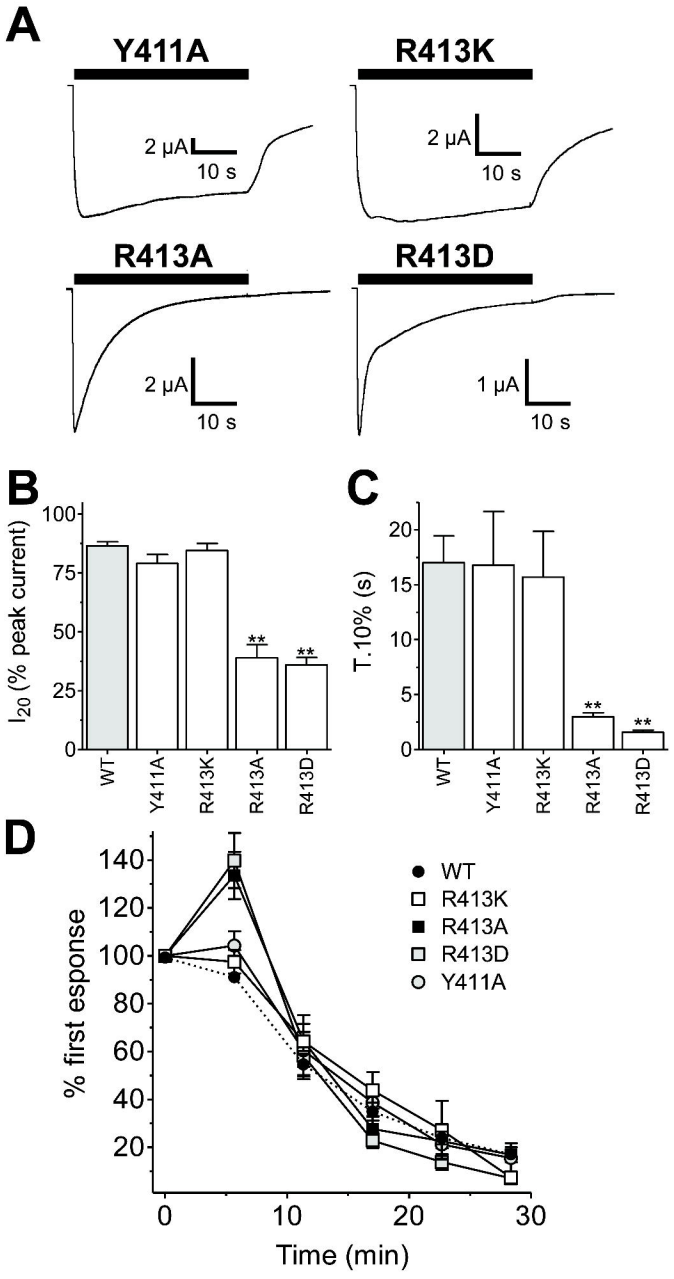
A
Y411A
2 μA
10 s
R413K
2 μA
10 s
R413A
2 μA
10 s
R413D
1 μA
10 s
B
I_{20} (% peak current)
100
75
50
25
0
**
**
WT
Y411A
R413K
R413A
R413D
C
T.10% (s)
20
15
10
5
0
**
**
WT
Y411A
R413K
R413A
R413D
D
% first esponse
140
120
100
80
60
40
20
0
10
20
30
Time (min)
WT
R413K
R413A
R413D
Y411A